

# α-Decay Half-Lives, α-Capture Cross Sections, and α-Nucleous Interaction

V. Yu. Denisov and A. A. Khudenko

Institute for Nuclear Research, Ukraine National Academy of Sciences, Kiev, UA-03680 Ukraine  
e-mail: denisov@kinr.kiev.ua

**Abstract**—The expression for the  $\alpha$ -nuclear potential was found. This potential describes the  $\alpha$ -decay half-lives for the ground states of nuclei and the  $\alpha$ -particle capture cross sections for  $^{40}\text{Ca}$ ,  $^{44}\text{Ca}$ ,  $^{59}\text{Co}$ ,  $^{208}\text{Pb}$ , and  $^{209}\text{Bi}$  nuclei well. The potential was used to calculate the probabilities of  $\alpha$ -transitions from the ground states of parent nuclei to different excited states of daughter nuclei. Simple analytical relations for calculating  $\alpha$ -decay half-lives for transitions between the ground states of nuclei are determined.

**DOI:** 10.3103/S1062873810040283

## INTRODUCTION

In more than one hundred years of studies, the  $\alpha$ -decay of nuclei and the  $\alpha$ -nucleous interaction have remained of interest [1–19]. At present, the process of the  $\alpha$ -decay of nuclei is used not only in experimental nuclear physics, but in technology and medicine. The number of papers devoted to the study of this process in the framework of microscopic, macroscopic–cluster, semi-microscopic models, fission model, and so on [3–10] grows with each passing year. Different empirical relations [11–14] have also been proposed that is very helpful in planning experiments. At present, there are a number of papers in which the processes of  $\alpha$ -decay and  $\alpha$ -capture by nuclei are described by one potential [3, 15]. We emphasize that the processes of  $\alpha$ -decay and  $\alpha$ -capture are reciprocal; it is therefore desirable to describe them by one potential, since capture cross section and decay half-life depend on the transmission coefficient of an  $\alpha$ -particle through the potential barrier.

The  $\alpha$ -nucleous interaction depends on deformations on the surface of the daughter nucleus that are determined by the parameters of quadrupole  $\beta_2$ - and hexadecapole  $\beta_4$  deformation, the mutual position of its axis of symmetry and  $\alpha$ -particle emission direction  $\theta$ , orbital momentum  $\ell$ , and the parity of the  $\alpha$ -transition. We propose the  $\alpha$ -nuclear potential found within the framework of the cluster model, which allows simultaneous calculation of the half-lives of  $\alpha$ -radioactive isotopes and the cross section of  $\alpha$ -capture by nuclei (a unified model for alpha decay and alpha capture, or UMADAC) [3]. Simple empirical relations are proposed for practical application in planning certain experimental measurements; these relations allow rapid estimations of the  $\alpha$ -decay half-life.

## α-NUCLEAR POTENTIAL, α-DECAY, AND α-CAPTURE

To construct the  $\alpha$ -nuclear potential, experimental data on  $\alpha$ -decay for transitions between ground states in 344 nuclei and  $\alpha$ -capture by  $^{40}\text{Ca}$ ,  $^{44}\text{Ca}$ ,  $^{59}\text{Co}$ ,  $^{208}\text{Pb}$ , and  $^{209}\text{Bi}$  in the neighborhood of the barrier were analyzed (see the references in [3]). Experimental values of spins and parities of nuclei, experimental and theoretical values of deformation parameters of daughter nuclei were also used. This potential allows us to find the  $\alpha$ -decay half-lives,

$$T_{1/2} = \frac{\hbar}{\Gamma(Q_\alpha, \ell)} = \frac{4\pi \ln 2}{\int 10^\nu t(Q_\alpha, \theta, \ell) d\Omega} \quad (1)$$

and the cross section of  $\alpha$ -capture by the nucleus [3],

$$\sigma = \frac{\pi \hbar^2}{2\mu E} \int_0^{\pi/2} \sum_{\ell} (2\ell + 1) t(E, \theta, \ell) \sin \theta d\theta. \quad (2)$$

Here,  $\Gamma(Q_\alpha, \ell)$  is the  $\alpha$ -decay width;  $10^\nu$  is a factor that takes into account the frequency of  $\alpha$ -particle collision with the barrier and its pre-production;  $\mu$  is the reduced mass;  $\ell$  is the orbital momentum of the  $\alpha$ -particle;  $E$  is collision energy of the  $\alpha$ -particle and the nucleus; and  $Q_\alpha$  is the energy released in the course of nucleus decay. The value of  $\nu \approx 19$  (see [3] for details).

The transmission coefficient of an  $\alpha$ -particle through the potential barrier is written as

$$t(Q_\alpha, \theta, \ell) = \frac{1}{1 + \exp \left[ \frac{2}{\hbar} \int_{a(\theta)}^{b(\theta)} dr \sqrt{2\mu(v(r, Q_\alpha, \theta, \ell) - Q_\alpha)} \right]}. \quad (3)$$

Here,  $a(\theta)$ ,  $b(\theta)$  are the inner and outer turning points found from the equality of the radicand to zero; and

$v(r, Q_\alpha, \theta, \ell)$  is the  $\alpha$ -nucleus interaction potential, which consists of the Coulomb, centrifugal, and nuclear parts, respectively:

$$v(r, Q_\alpha, \theta, \ell) = v_C(r, \theta) + v_N(r, Q_\alpha, \theta) + v_\ell(r). \quad (4)$$

The nuclear part of the  $\alpha$ -nucleus interaction potential is selected in the form

$$v_N(r, Q_\alpha, \theta) = \frac{V(Q_\alpha)}{1 + \exp[(r - r_c(\theta))/d]}, \quad (5)$$

where  $V(Q_\alpha), r_c(\theta) = 1.1683 + R(1 + \beta_2 Y_{20}(\theta) + \beta_4 Y_{40}(\theta))$  are the depth of the nuclear part of the potential and the effective radius, respectively;  $R = 1.2915A^{1/3}(1 + 1.4088/A - 0.0994(A - 2Z)/A)$  is the parameter of radius of the daughter nucleus; and  $A$  and  $Z$  are the numbers of nucleons and protons in the nucleus. The radius of the interaction potential depends on the parameters of quadrupole and hexadecapole deformations of the daughter nucleus. The Coulomb and the centrifugal parts of the  $\alpha$ -nuclear potential are

$$\begin{aligned} v_C(r, \theta) &= \frac{2Ze^2}{r} \left( 1 + \frac{3R^2}{5r^2} \beta_2 Y_{20}(\theta) + \frac{3R^4}{9r^4} \beta_4 Y_{40}(\theta) \right) \\ &\text{for } r \geq r_c(\theta), \\ v_C(r, \theta) &= \frac{2Ze^2}{r_c(\theta)} \left( \frac{3}{2} - \frac{r^2}{2r_c(\theta)^2} \right. \\ &+ \frac{3R^2}{5r_c(\theta)^2} \beta_2 Y_{20}(\theta) \left( 2 - \frac{r^3}{2r_c(\theta)^3} \right) \\ &+ \left. \frac{3R^4}{9r_c(\theta)^4} \beta_4 Y_{40}(\theta) \left( \frac{7}{2} - \frac{5r^2}{2r_c(\theta)^2} \right) \right) \text{ for } r \leq r_c(\theta), \\ v_\ell(r) &= \frac{\hbar^2 \ell(\ell+1)}{2\mu r^2}. \end{aligned} \quad (6)$$

Here,  $e$  is the proton charge and  $Y_{20}(\theta)$  and  $Y_{40}(\theta)$  are the spherical harmonic functions.

The emission of an  $\alpha$ -particle by the nucleus takes place according to spin and parity selection rules

$$|I_i - I_j| \leq \ell_\alpha \leq I_i + I_j, \quad P_i/P_j = (-1)^{\ell_\alpha}, \quad (8)$$

where  $I_i$  and  $I_j$  are the spins of the parent and daughter nuclei; and  $P_i$  and  $P_j$  are their parities, respectively. It is assumed for the sake of simplicity that the transitions take place for the minimum possible value of orbital momentum. The value of  $Q_\alpha$  is associated with the mass defects of the parent  $\Delta M_p$ , daughter  $\Delta M_d$  nuclei, and  $\alpha$ -particle  $\Delta M_\alpha$ , respectively:

$$Q_\alpha = \Delta M_p - (\Delta M_d + \Delta M_\alpha) + k(Z_p^\epsilon - Z_d^\epsilon). \quad (9)$$

The last term in (9) takes into account the screening of the nucleus by electrons:  $k = 8.7$  eV,  $\epsilon = 2.517$  for nuclei with  $Z \geq 60$  and  $k = 13.6$  eV, and  $\epsilon = 2.408$  for nuclei with  $Z < 60$ .

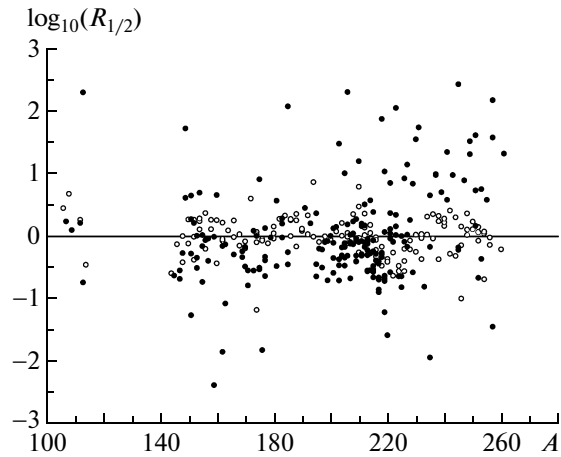


**Fig. 1.** Difference between common logarithms of experimental and theoretical values of  $\alpha$ -decay half-lives ( $R_{1/2}$ ) as a function of mass number  $A$ . Bullets correspond to even-odd, odd-even, and odd-odd nuclei; open circles correspond to even-even nuclei.

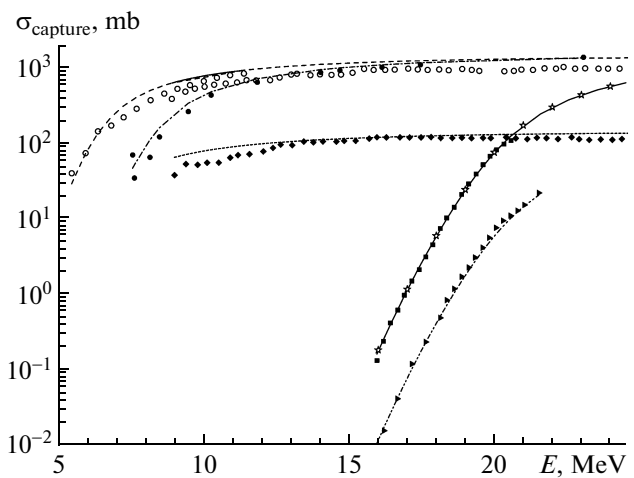


**Fig. 2.** Comparison of experimental excitation functions for  $\alpha$ -particle capture cross sections for (open circles)  ${}^{40}\text{Ca}$ , (diamonds)  ${}^{44}\text{Ca}$ , (bullets)  ${}^{59}\text{Co}$ , (squares)  ${}^{208}\text{Pb}$ , and (triangles)  ${}^{209}\text{Bi}$  with theoretical functions. Theoretical cross sections for (dashed line)  ${}^{40}\text{Ca}$ , (long/short dashed line)  ${}^{44}\text{Ca}$ , (dashed/dotted line)  ${}^{59}\text{Co}$ , (solid line)  ${}^{208}\text{Pb}$ , and (dash/double-dotted line)  ${}^{209}\text{Bi}$  found within the UMADAC framework. Stars show the calculated  $\alpha$ -particle capture cross sections by  ${}^{208}\text{Pb}$  within the framework of the coupled channels model. The values for cross sections of  $\alpha + {}^{59}\text{Co}$  and  $\alpha + {}^{208}\text{Pb}$  are reduced by a factor of 10 for better representation.

The parameters of  $\alpha$ -nucleus interaction [3] were determined from fitting the experimental values for the half-lives in 344 nuclei and the capture cross section of an  $\alpha$ -particle by  ${}^{40}\text{Ca}$ ,  ${}^{44}\text{Ca}$ ,  ${}^{59}\text{Co}$ ,  ${}^{208}\text{Pb}$ , and  ${}^{209}\text{Bi}$  nuclei. The obtained potential was then used to calculate the half-lives for 902 potentially possible

**Table 1.** Comparison of experimental and theoretical probabilities of  $\alpha$ -transitions from the ground state of a parent nucleus to the ground and excited states of a daughter nucleus

Transition	$Q$ , MeV	$B_i^{\text{exp}}$ , %	$B_i^{\text{theor}}$ , %	Transition	$Q$ , MeV	$B_i^{\text{exp}}$ , %	$B_i^{\text{theor}}$ , %
$^{222}\text{Ra} \rightarrow ^{218}\text{Rn}$							
$0^+ \rightarrow 0^+$	6.7136	96.90	96.70	$0^+ \rightarrow 0^+$	5.4513	68.15	69.00
$0^+ \rightarrow 2^+$	6.3896	3.05	3.27	$0^+ \rightarrow 2^+$	5.3935	31.55	27.60
$0^+ \rightarrow (4^+)$	6.0608	0.0041	0.0634	$0^+ \rightarrow 4^+$	5.2645	0.3	3.34
$^{224}\text{Ra} \rightarrow ^{220}\text{Rn}$							
$0^+ \rightarrow 0^+$	5.8242	94.92	95.70	$0^+ \rightarrow 0^+$	4.8954	71.38	71.00
$0^+ \rightarrow 2^+$	5.5832	5.06	4.22	$0^+ \rightarrow 2^+$	4.8422	28.42	26.40
$0^+ \rightarrow 4^+$	5.2905	0.0073	0.0596	$0^+ \rightarrow 4^+$	4.7213	0.2	2.60
$^{226}\text{Ra} \rightarrow ^{222}\text{Rn}$							
$0^+ \rightarrow 0^+$	4.9058	94.45	95.80	$0^+ \rightarrow 0^+$	4.6109	74.00	71.50
$0^+ \rightarrow 2^+$	4.7196	5.55	4.18	$0^+ \rightarrow 2^+$	4.5614	26.00	26.00
$0^+ \rightarrow 4^+$	4.4574	0.0065	0.03	$0^+ \rightarrow 4^+$	4.4486	0.15	2.44
$^{226}\text{Th} \rightarrow ^{222}\text{Ra}$							
$0^+ \rightarrow 0^+$	6.4876	75.50	76.40	$0^+ \rightarrow 0^+$	4.3078	79.00	74.10
$0^+ \rightarrow 2^+$	6.3765	22.80	21.40	$0^+ \rightarrow 2^+$	4.2582	21.00	24.10
$0^+ \rightarrow 4^+$	6.1862	0.19	2.06	$0^+ \rightarrow 4^+$	4.1448	0.078	1.72
$^{228}\text{Th} \rightarrow ^{224}\text{Ra}$							
$0^+ \rightarrow 0^+$	5.5565	72.20	76.30	$0^+ \rightarrow 0^+$	5.0235	76.49	67.20
$0^+ \rightarrow 2^+$	5.4721	27.20	21.90	$0^+ \rightarrow 2^+$	4.9786	23.48	28.70
$0^+ \rightarrow 4^+$	5.3057	0.23	1.65	$0^+ \rightarrow 4^+$	4.8751	0.03	3.88
$^{230}\text{Th} \rightarrow ^{226}\text{Ra}$							
$0^+ \rightarrow 0^+$	4.8065	76.30	76.70	$0^+ \rightarrow 0^+$	5.9420	76.90	60.30
$0^+ \rightarrow 2^+$	4.7388	23.40	21.90	$0^+ \rightarrow 2^+$	5.8992	23.10	31.90
$0^+ \rightarrow 4^+$	4.5950	0.12	1.36	$0^+ \rightarrow 4^+$	5.8003	0.02	7.14
$^{230}\text{U} \rightarrow ^{226}\text{Th}$							
$0^+ \rightarrow 0^+$	6.0308	67.40	68.80	$0^+ \rightarrow 0^+$	6.2586	84.20	60.00
$0^+ \rightarrow 2^+$	5.9586	32.00	26.20	$0^+ \rightarrow 2^+$	6.2152	15.70	32.00
$0^+ \rightarrow 4^+$	5.8044	0.38	3.09	$0^+ \rightarrow 4^+$	6.1150	0.24	7.27

$\alpha$ -radioactive nuclei tabulated in [3]. This potential allowed us to describe even-even, even-odd, odd-even, and odd-odd nuclei over a wide range of mass numbers by a unified set of parameters.

The mean-square errors of common logarithms of  $\alpha$ -decay half-lives

$$\delta = \sqrt{\frac{1}{N} \sum_{k=1}^N \left[ \log_{10}(T_{1/2}^{\text{theor}}) - \log_{10}(T_{1/2}^{\text{exp}}) \right]^2} \quad (10)$$

found within the framework of our model are lower than the values calculated in other models. In (10),  $N$  is the total number of nuclei for which the  $\alpha$ -decay half-lives are known.

The difference between the experimental and theoretical values of common logarithms for half-lives of

$\alpha$ -radioactive isotopes depending on the mass number is shown in Fig. 1. Figure 2 shows the theoretical curves and experimental points of energy dependences of cross sections of  $\alpha$ -particle capture by  $^{40}\text{Ca}$ ,  $^{44}\text{Ca}$ ,  $^{59}\text{Co}$ ,  $^{208}\text{Pb}$ , and  $^{209}\text{Bi}$  nuclei.

## EMPIRICAL RELATIONS

The experimental data for half-lives of 344 nuclei and experimental information on the spins and parities of the ground states of nuclei were used in finding the empirical dependences of the half-life of  $\alpha$ -radioactive nuclei on the mass number, nuclear charge, the value of  $Q_\alpha$ , and the orbital momentum of the  $\alpha$ -particle. Analysis was performed for the complete set of 344 nuclei, and separately for light ( $Z \leq 82$ ,  $A \leq 208$ )

**Table 2.** Comparison of experimental and theoretical probabilities of α-transitions from the ground state of a parent nucleus to the ground and excited states of a daughter nucleus. Theoretical calculations are performed within the UMADAC framework and the models in [16–18]

Transition	$Q$ , MeV	$B_i^{\text{exp}}$ , %	$B_i^{\text{theor}}$ , %	$B_i$ , % [16]	$B_i$ , % [17]	$B_i$ , % [18]
$^{238}\text{Pu} \rightarrow ^{234}\text{U}$	$0^+ \rightarrow 0^+$	5.6322	70.90	62.00	75.57	77.41
	$0^+ \rightarrow 2^+$	5.5887	28.98	31.20	23.00	21.52
	$0^+ \rightarrow 4^+$	5.4888	0.11	6.28	1.41	1.06
	$0^+ \rightarrow 6^+$	5.3361	0.003	0.492	0.0176	$9.3 \times 10^{-3}$
	$0^+ \rightarrow 8^+$	5.1352	$6.8 \times 10^{-6}$	0.0144	$4.40 \times 10^{-5}$	$1.41 \times 10^{-5}$
	$0^+ \rightarrow 0^+$	4.8223	$5 \times 10^{-5}$	$3.22 \times 10^{-4}$	$3.65 \times 10^{-5}$	$8.00 \times 10^{-5}$
	$0^+ \rightarrow 0^-$	4.5877	$1.2 \times 10^{-6}$	$7.38 \times 10^{-8}$	$2.89 \times 10^{-7}$	$9.00 \times 10^{-7}$
	$0^+ \rightarrow 0^+$	6.2559	74.08	59.00	74.00	76.00
$^{242}\text{Cm} \rightarrow ^{228}\text{Pu}$	$0^+ \rightarrow 2^+$	6.2118	25.92	32.30	24.20	22.70
	$0^+ \rightarrow 4^+$	6.1099	$3.5 \times 10^{-2}$	7.85	1.765	1.333
	$0^+ \rightarrow 6^+$	5.9525	$4.6 \times 10^{-3}$	0.82	$2.8 \times 10^{-3}$	$1.52 \times 10^{-2}$
	$0^+ \rightarrow 8^+$	5.7423	$2.0 \times 10^{-5}$	$3.45 \times 10^{-2}$	$10^{-4}$	$3.2 \times 10^{-5}$
$^{246}\text{Cf} \rightarrow ^{242}\text{Cm}$	$0^+ \rightarrow 0^+$	6.9032	79.30	55.90	71.60	73.90
	$0^+ \rightarrow 2^+$	6.8611	20.60	33.00	25.90	24.30
	$0^+ \rightarrow 4^+$	6.7662	0.15	9.79	2.43	1.82
	$0^+ \rightarrow 6^+$	6.6152	0.016	1.35	0.061	0.032

and heavy nuclei. It was shown that the empirical expression

$$\log_{10}(T_{1/2}) = a_1 + a_2 \frac{A^{1/6} Z^{1/2}}{(A/(A-4))^{1/6}} + a_3 \frac{Z}{\sqrt{Q_\alpha}} + a_4 A^{1/6} \frac{\sqrt{\ell(\ell+1)}}{Q_\alpha} + a_5 ((-1)^\ell - 1) \quad (11)$$

results in small values of mean-square errors (10) and describes well the transitions between the ground states of even–even, even–odd, odd–even, and odd–odd nuclei [4]. The parameters  $a_i$ ,  $i = 1, 5$  which are different for even–even, even–odd, odd–even, and odd–odd nuclei, are given in [4].

### α-TRANSITIONS FROM THE GROUND STATE OF A PARENT NUCLEUS TO EXCITED STATES OF A DAUGHTER NUCLEUS

The  $\alpha$ -nuclear potential found within the framework of the UMADAC cluster model allows us to estimate the half-lives for transitions between the ground states of parent and daughter nuclei and the  $\alpha$ -decay half-lives for transitions between different excited states of parent and daughter nuclei without the introduction of additional fitting parameters. The value of energy released in the case of an  $\alpha$ -transition from the state of parent nucleus  $E_{jp}$  to the state of daughter nucleus  $E_{id}$  is

$$Q_{i \rightarrow j} = Q_{\text{oc} \rightarrow \text{oc}} + E_{jp} - E_{id}. \quad (12)$$

The high excited nuclear levels have a complex structure; the transitions between the ground state of the parent nucleus and the low excited states of the daughter nucleus for even number of protons and neutrons belonging to the main rotational band were therefore analyzed. In this case, the contribution of microscopic effects due to the complex structure of the excited level into the  $\alpha$ -decay is small.

The relative probability of a transition from the ground state of a parent nucleus to the excited state of a daughter nucleus is estimated using the expression

$$B_i = \frac{\Gamma(Q_b, \ell_i)}{\sum_n \Gamma(Q_b, \ell_n)} \times 100\% = \frac{P(Q_b, \ell_i)}{\sum_n P(Q_b, \ell_n)} \times 100\%, \quad (13)$$

where  $\Gamma(Q_b, \ell_i), P(Q_b, \ell_i) = \int t(Q_b, \theta, \ell) d\Omega$  is the level width (see (1)) and the probability of penetration of the  $\alpha$ -particle through the potential barrier, respectively.

The results from calculating the probabilities for low levels of the main rotational band are given in Table 1. The results from calculations within the framework of our model are compared with the corresponding results from calculations of transition probabilities within the framework of other approaches in Table 2. With increasing energy levels of the daughter nucleus, the theoretical value of the transition probability begins to deviate from the experimental value. The reason for this discrepancy is that (a) different microscopic factors associated with the formation of an  $\alpha$ -particle in a daughter nucleus and (b) the micro-

scopic structure of the excited state, which differs considerably from the structure of the ground state, are ignored.

## CONCLUSIONS

We have constructed an UMADAC model that allows us to simultaneously describe  $\alpha$ -decay from the ground state of a parent nucleus to the ground and low excited states of a daughter nucleus, and the capture cross section of an  $\alpha$ -particle by the nuclei. The parameters of the  $\alpha$ -nuclear potential were obtained, and the half-lives for 902  $\alpha$ -radioactive isotopes whose decay was not experimentally detected were estimated. Simple empirical dependences that take into account the momentum of the  $\alpha$ -transition and the parity of nuclei were found for the half-lives of even-even, even-odd, odd-even, and odd-odd nuclei unstable with respect to  $\alpha$ -decay.

## REFERENCES

1. Gamow, G., *Z. Phys.*, 1928, vol. 51, p. 204.
2. Condon, E.U. and Gurney, R.W., *Nature*, 1928, vol. 122, p. 439.
3. Denisov, V.Yu. and Khudenko, A.A., *Atomic Data and Nucl. Data Tables*, 2009, vol. 95, p. 815.
4. Denisov, V.Yu. and Khudenko, A.A., *Phys. Rev. C*, 2009, vol. 79, p. 054614.
5. Stewart, T.L., et al., *Nucl. Phys. A*, 1996, vol. 611, p. 332.
6. Buck, B., Merchant, A.C.M., and Perez, S., *J. Phys. G*, 1991, vol. 17, p. 1223; *Phys. Rev. C*, 1992, vol. 45, p. 2247; *Atomic Data and Nucl. Data Tables*, 1993, vol. 54, p. 53.
7. Moustabchir, R. and Royer, G., *Nucl. Phys. A*, 2001, vol. 683, p. 266.
8. Chang, Xu and Zhongzhou, R., *Phys. Rev. C*, 2006, vol. 73, p. 041301.
9. Medeiros, E.L., et al., *J. Phys. G*, 2006, vol. 32, p. B23.
10. Duarte, S.B., et al., *Atomic Data and Nucl. Data Tables*, 2002, vol. 80, p. 235.
11. Dasgupta-Schubert, N. and Reyes, M.A., *Atomic Data and Nucl. Data Tables*, 2007, vol. 93, p. 907.
12. Gupta, M. and Burrows, T.W., *Nucl. Data Sheets*, 2005, vol. 106, p. 251.
13. Poenaru, D.N., Plonski, I.H., and Greiner, W., *Phys. Rev. C*, 2006, vol. 74, p. 014312.
14. Viola, V.E. and Seaborg, G.T., *Inorg. J. Nucl. Chem.*, 1966, vol. 28, p. 741.
15. Denisov, V.Yu. and Ikezoe, H., *Phys. Rev. C*, 2005, vol. 72, p. 064613.
16. Wang, Y.Z., Zhang, H.F., Dong, J.M., and Royer, G., *Phys. Rev. C*, 2009, vol. 79, p. 014316.
17. Chang Xu and Zhongzhou Ren, *Nucl. Phys. A*, 2006, vol. 778, p. 1.
18. Preston, M.A., *Phys. Rev.*, 1947, vol. 71, p. 865.
19. <http://www.nds.iaea.org/RIPL-2/>